A 1.3/1.55-μm Wavelength-Division Multiplexing Optical Module Using a Planar Lightwave Circuit for Full Duplex Operation

Toshikazu Hashimoto, Takeshi Kurosaki, Masahiro Yanagisawa, Yasuhiro Suzuki, *Member, IEEE*, Yuji Akahori, Yasuyuki Inoue, *Member, IEEE*, Yuichi Tohmori, *Member, IEEE*, Kazutoshi Kato, *Member, IEEE*, Yasufumi Yamada, Noboru Ishihara, and Kuniharu Kato, *Member, IEEE*

***Abstract*—We developed a hybrid integrated optical module for 1.3/1.55-μm wavelength-division multiplexing (WDM) full-duplex operation. The optical circuit was designed to suppress the optical and electrical crosstalk using a wavelength division multiplexing filter. And an optical crosstalk of −43 dB and an electrical crosstalk of −105 dB were achieved with a separation between the transmitter laser diode and the receiver photodiode of more than 9 mm. We used the optical circuit design to fabricate an optical module with a bare chip preamplifier in a package. This module exhibited a full duplex operation of 156 Mbit/s with a minimum sensitivity of −35.2 dBm at a bit error rate of 10^{-10}.**

***Index Terms*—Electrical crosstalk, full-duplex operation, optical crosstalk, optical hybrid integration, optical transceiver module, passive optical network (PON), planar lightwave circuit platform.**

I. Introduction

FULL-DUPLEX optical modules are key devices for 1.3/1.55-μm bidirectional wavelength-division multiplexing (WDM) optical subscriber systems and reducing their cost is particularly important [1]. We have already developed an optical module for use in the optical network units of synchronous transfer mode passive optical networks (STM-PONs) by using planar lightwave circuit (PLC) platform technology [2], [3]. The module cost is lower than that of conventional optical modules because we have integrated its optical functions and simplified its assembly. The module includes a 1.3/1.5-μm WDM splitter, an optical Y-branch circuit, a transmitter laser diode (LD) and a receiver photodiode (PD) on a 3×15 mm planar waveguide substrate. With full duplex operation, the receiver performance is degraded by optical and electrical crosstalk from the LD, which is integrated near the PD in a small area. This becomes a severe problem, especially for asynchronous transfer mode passive optical networks (ATM-PON)[4], which require high receiver sensitivity for full duplex operation. With a view to realizing a full duplex operation optical transceiver for 1.3/1.55 μm bidirectional WDM optical subscriber systems, we propose an optical circuit configuration designed to suppress the optical and electrical crosstalk from the LD to the PD, and optimize the optical circuit by experiments and simple calculations. In Section II, we propose an optical circuit configuration for an optical transceiver module for the ATM-PON using PLC platform technology. In Section III, we evaluate the crosstalk criterion for the ATM-PON specification. Finally, we describe module fabrication and performance in Sections IV and V, respectively.

Manuscript received July 11, 2000; revised August 3, 2000.

T. Hashimoto, M. Yanagisawa, Y. Akahori, Y. Inoue, Y. Yamada, K. Kato are with the NTT Photonics Laboratories, Shirakata, Tokai, Naka, Ibaraki 319-1193, Japan (e-mail: hasimoto@iba.iecl.ntt.co.jp).

T. Kurosaki, Y. Suzuki, Y. Tohmori, K. Kato, and N. Ishihara are with the Morinosato, Atsugi, Kanagawa 243-0198, Japan.

Publisher Item Identifier S 0733-8724(00)09822-4.

II. Proposed Optical Circuit Configuration

Fig. 1 shows the single fiber ATM-PON system that is the application target of our optical module. Our module is used as an optical transceiver called an optical network unit (ONU) or optical line terminal (OLT). The ATM-PON employs an optical WDM signal in which 1.3 and 1.55 μm wavelength lights are used for the upstream and downstream signals, respectively. To utilize the WDM system, the transceiver must be capable of full duplex operation in addition to having a WDM circuit. The system has a passive double star (PDS) configuration to accommodate many subscribers. The optical module for this configuration is required to have a high optical output power and a high sensitivity since it has to receive a divided signal from an optical splitter. Therefore, we must suppress the crosstalk from the transmitter LD to the receiver PD caused by the high output power operation, to achieve high sensitivity in full duplex operation. The crosstalk between the LD and the PD in a module can be divided into optical crosstalk and electrical crosstalk. For an integrated optical transceiver module, the LD and PD are assembled in a small area, and the optical crosstalk is caused by uncoupled stray light from the LD at the LD-waveguide butt coupling. Therefore, we designed an optical circuit using a PLC platform to isolate the PD from the stray light with a 1.3/1.55 μm WDM filter [5]. Fig. 2 shows the optical module configuration. In an ONU for ATM-PON, 1.3 and 1.55 μm wavelength lights are used as output and input lights, respectively. The circuit consists of a 1.3/1.5 μm WDM circuit, a 1.3 μm LD, a 1.3 μm PD as a power monitor photodiode (M-PD) for the LD, and a 1.55 μm receiver PD (R-PD). The WDM circuit is composed of a silica waveguide and a WDM film inserted in a groove formed on the waveguide. The film, which is fixed in the groove with an adhesive, reflects 1.3 μm light and allows 1.55 μm light to pass. The LD and PDs are flip-chip-bonded on the silicon terrace of the PLC platform [6], and encapsulated in a transparent silicone resin.

This configuration has two advantages as regards reducing both the electrical and optical crosstalk between the LD and

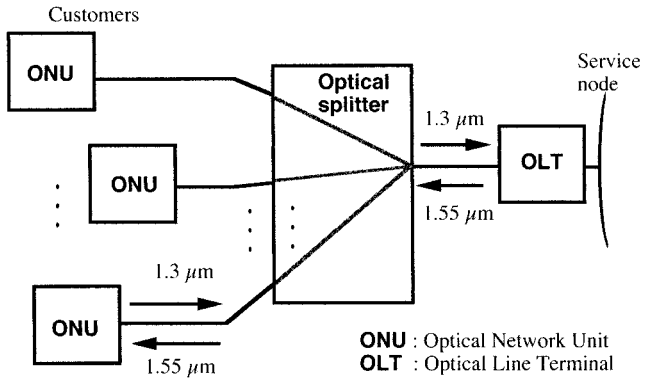

Fig. 1. ATM passive double star system configuration.

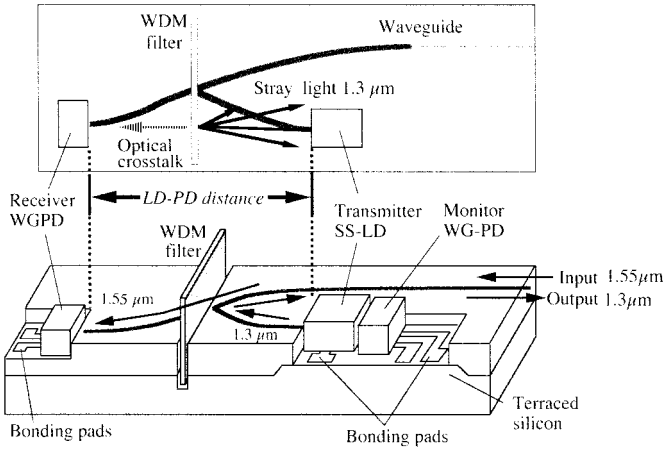

Fig. 2. Full duplex 1.3/1.55 μm WDM optical module configuration with PLC platform.

R-PD. First, the WDM filter optically isolates the R-PD from the LD by reflecting uncoupled stray light from the LD as well as the output signal light. This reduces the optical crosstalk directly. Second, the LD and PD are separated on the small substrate by placing the LD on the opposite side of the WDM filter to the PD. This effectively reduces the electrical and optical crosstalk because the crosstalk decreases greatly with distance.

III. Crosstalk Estimation

To fabricate an optical module with the above configuration, we first determined the LD-PD distance by investigating the relationship between distance and optical and electrical crosstalk. We fabricated three types of optical module with LD-PD distances of 6, 9, and 14 mm for the experiment. In all the modules, the LDs and R-PDs were encapsulated in a transparent silicone resin in the same way as an actual module. We used a WDM filter, which had an isolation of more than 50 dB between 1.3 and 1.55 μm.

Fig. 3 shows the relationship between optical crosstalk and LD-PD distance before and after WDM filter installation. The optical crosstalk X_{opt} [dB] is defined as

$$X_{opt} = 10 \log_{10}\left(\frac{I_x/\alpha}{P_t}\right) = 10 \log_{10}(P_r/P_t) \quad (1)$$

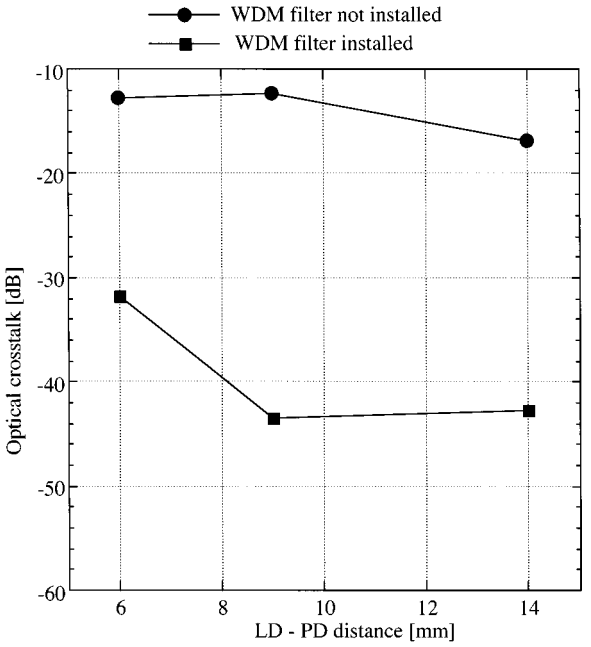

Fig. 3. Relationship between LD-PD distance and optical crosstalk.

where

P_t[mW]	module output power;
I_x[mA]	photo current with no input signal caused by stray light from the transmitter LD when the module output power is P_t;
α[A/W]	responsivity of the module;
P_r[mW]	estimated received optical crosstalk noise power defined as $P_r = I_x/\alpha$.

The optical crosstalk was effectively suppressed by the WDM filter and was less than -43 dB when the LD-PD distance was more than 9 mm. The improvement range of 20–30 dB was not identical to the WDM filter isolation of 50 dB and the suppression of the optical crosstalk was saturated at distances greater than 9 mm. This is because the stray light, which propagated unhindered through the waveguide cladding, was randomly reflected at the WDM filter and passed through it with a large incident angle. In this case, the optical crosstalk was almost independent of the LD-PD distance. When the LD-PD distance was 6 mm, the stray light included other propagating lights in addition to the cladding mode and this also propagated to the filter while it was eliminated at greater distances.

Fig. 4 shows the relationship between the electrical crosstalk and the LD-PD distance. The measurement was carried out with 50 Ω impedance matching as shown in Fig. 5. The electrical crosstalk X_{elec} [dB] is defined as

$$X_{elec} = 20 \log_{10}(V_r/V_t) \quad (2)$$

where V_t [V] is the applied voltage at the LD signal port, and V_r [V] is the measured voltage at the loaded resistance to the PD. When the LD-PD distance was more than 9 mm, the crosstalk was below -100 dB at 130 MHz.

Since the optical and electrical crosstalk occur simultaneously during a full duplex operation, the total crosstalk affects the module sensitivity. To estimate the total crosstalk, we use the

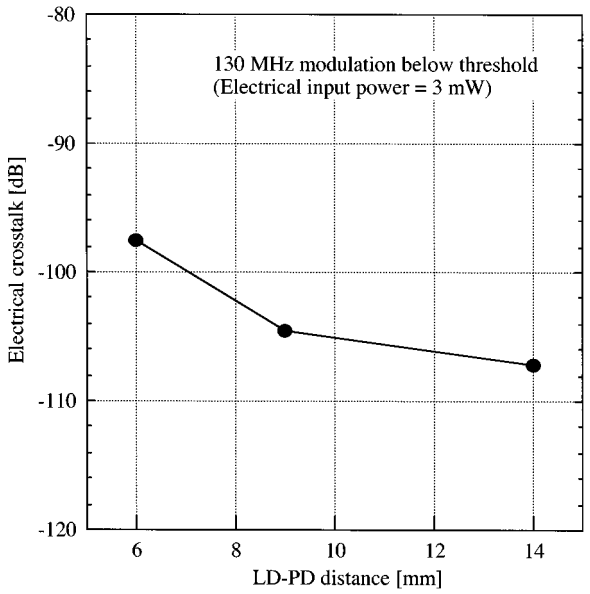

Fig. 4. Relationship between LD-PD distance and electrical crosstalk.

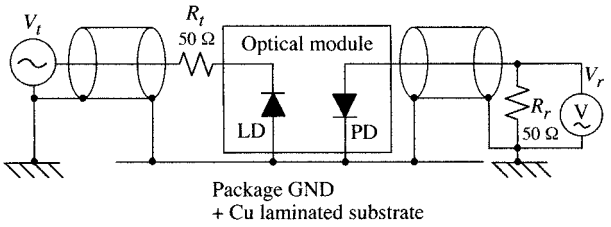

Fig. 5. Electrical crosstalk measurement system.

calculation below to convert the electrical crosstalk into equivalent optical crosstalk.

The module output power P_t at an applied voltage V_t is described as $P_t = \eta V_t/R_t$, where R_t [Ω] is the resistance of the transmitter part, and η [W/A] is the efficiency of the module output power against the injection current. The electrical crosstalk voltage V_r corresponds to the electrical signal caused by the equivalent optical signal power P_r^* [W] defined as $P_r^* = (1/\alpha)V_r/R_r$. The equivalent optical crosstalk X_{opt}^* of the electrical crosstalk is reduced by substituting the equivalent optical signal power of the electrical crosstalk P_r^* for the optical crosstalk noise P_r in (1). By using these equations, the relationship between the electrical crosstalk and the equivalent optical crosstalk is described as

$$X_{opt}^* = X_{elec}/2 + 10\log_{10}[(1/\alpha\eta)R_t/R_r]. \qquad (3)$$

Fig. 6 shows this relation. Here the other parameters are set at $\eta = 0.1$ W/A, $\alpha = 0.65$ A/W and $R_t = 50\ \Omega$. In actual use, the module includes a preamplifier, which has $R_r \approx 1$ kΩ impedance, while the crosstalk was measured with $R_r = 50\ \Omega$. Therefore, the measurement value should be converted using the loaded resistance. When the distance between LD and the R-PD was more than 9 mm, the equivalent optical crosstalk was more than -41 dB for 130 MHz operation at $R_r = 50\ \Omega$. This value is estimated to be -54 dB for actual use by converting from the $R_r = 50\ \Omega$ point (square) to the $R_r = 1$ kΩ point (circle). The

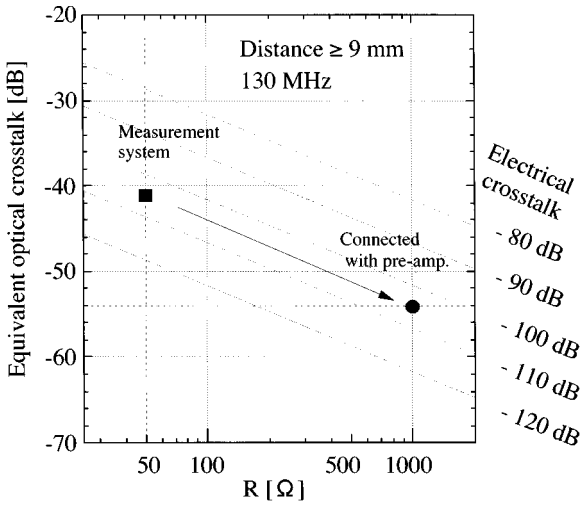

Fig. 6. Conversion chart from electrical crosstalk to equivalent optical crosstalk.

equivalent optical crosstalk of -54 dB is much smaller than the actual value of -43 dB and this means that the optical crosstalk is dominant when this module used practically.

Using Figs. 3–6, we can estimate the total crosstalk $X_{tot} = X_{opt} + X_{opt}^*$ for a given LD-PD distance.

Next we evaluate the total allowable crosstalk noise power range for the required minimum sensitivity for full duplex operation. With the simple calculation given in the Appendix, the minimum sensitivity for full duplex operation is obtained from the minimum sensitivity without LD operation and the total crosstalk noise power [see (7)]. Here, we calculated the total crosstalk noise power P_X [dBm] by using the optical output power P_t [dBm] and the total crosstalk X_{tot} [dB] as $P_X = P_t + X_{tot}$. This relationship is shown in Fig. 7 as a contour plot of the minimum sensitivity for full duplex operation (contour line) to the minimum sensitivity without LD operation (vertical axis) and the total crosstalk noise power (horizontal axis). In the calculation, the bit error rate (BER) is fixed at 10^{-10} which corresponds to the ATM-PON system requirements. Using the chart, we can estimate the allowable crosstalk power as described below. When, for example, we require a minimum sensitivity of -33 dBm for duplex operation, we start at -33 dBm (open circle) on the left side vertical axis and move along the contour line (thick curve). And if we can accept a power penalty of 1 dB, we stop at the point 1 dB below the starting point (open square) and read the total crosstalk power value at the point indicated by the dotted line with the arrow. Then, the allowable crosstalk power range is determined as being below the total crosstalk power value, which is below -40 dBm in this case. As another example, when the minimum sensitivity without LD operation is given, the allowable total crosstalk power is shown by the left side region from the point of the given minimum sensitivity without LD operation on the contour line of the required minimum sensitivity. For example, when the minimum sensitivity without LD operation is -40 dBm and we require a minimum sensitivity of -33 dBm for full-duplex operation, the acceptable maximum crosstalk power point is the filled square on the -33 dBm contour line.

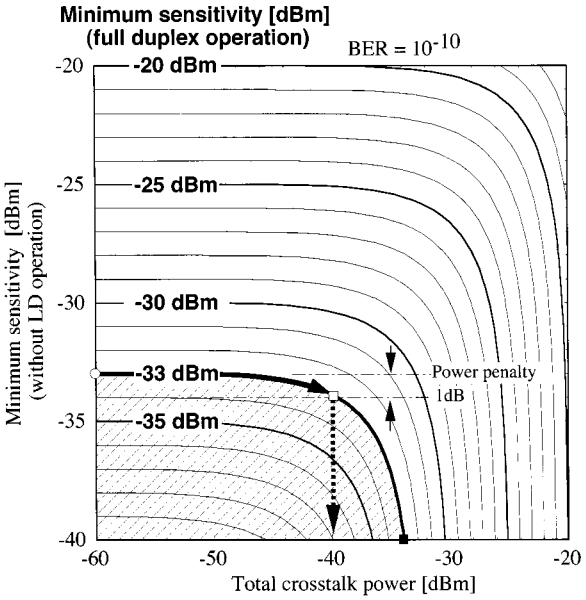

Fig. 7. Minimum sensitivity for full duplex operation against minimum sensitivity without LD operation and crosstalk noise power.

IV. Optical Module Fabrication

The average optical output power and the minimum sensitivity of the optical module are specified as 2 and −33 dBm, respectively, in the class C specification of the ATM-PON system [4]. Considering the above relation between the crosstalk power and the minimum sensitivity and the required performance of the module, we set our target optical crosstalk value at less than −42 dB. This provides a power penalty of less than 1 dB for a sensitivity value of −34 dBm. This crosstalk value means that the LD-PD distance must be more than 9 mm based on Fig. 3 since the optical crosstalk is the dominant crosstalk in our optical module. We determined 14 mm to be the distance needed to ensure that we achieved the above crosstalk value. We then fabricated an optical module using this LD-PD distance. The module configuration was identical to that described in Section II. The waveguide of the module had a 7 $\times$7 μm core with a refractive index difference of 0.45%. The substrate was 2.5 $\times$ 20 mm. A 1.3 μm spot size converter integrated laser diode (SS-LD) [7] was used as a transmitter LD and a 1.3 μm waveguide photodiode (WGPD) [8] was used as a power monitor photodiode (M-PD) for the LD. We used a 1.5 μm WGPD for the receiver PD (R-PD). All the optical semiconductor chips were flip-chip bonded on the PLC platform with AuSn solder. The R-PD wiring was formed on the undercladding to reduce the parasitic capacitance [9]. We inserted a WDM filter in a slot, 20 μm wide and 150 μm deep, that we formed in the PLC platform substrate using a diamond dicing saw, and fixed it in place with an epoxy adhesive. The filter was a dielectric multilayer film formed on a polyimide film [5]. The PLC substrate was fixed in a ceramic package (Fig. 8). A trans-impedance amplifier [10] was also installed in the package. The R-PD pad formed on the undercladding of the PLC platform and trans-impedance amplifier were connected with wire bonding, less than 1 mm in length, to reduce the parasitic capacitance. The LD and M-PD electrodes and the ceramic package were also connected with a short wire. After wire bonding, the LD, the PDs and the amplifier IC were encapsulated in a transparent silicone resin. A single-mode optical fiber was connected to the PLC.

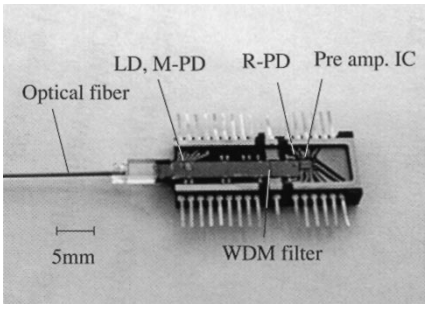

Fig. 8. Photograph of module housed in ceramic package with preamplifier IC.

TABLE I
Module Characteristics

Transmitter	Operating wavelength	1.3 μm
	Threshold	7 mA
	LD driving current at 5 dBm CW output power	43 mA
	Power deviation in APC during operation between -20℃ and 70 ℃	1.0 dB
Receiver	Operating wavelength	1.55 μm
	Responsivity (without pre amp. IC)	0.65 A/W
	Capacitance (without pre amp. IC)	0.7 pF
Optical crosstalk		-44 dB
Minimum sensitivity	LD inactivated operation	-35.9 dBm
	Full duplex operation	-35.2 dBm

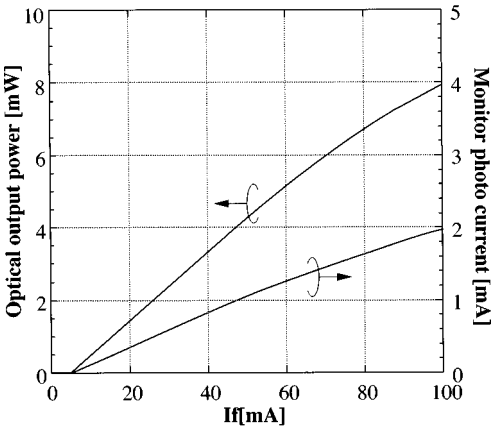

Fig. 9. Module output light power.

V. Optical Module Performance

We measured the performance of the module. The characteristics are summarized in Table I. Fig. 9 shows a typical optical output power against injection current during CW operation. The driving current for a 5-dBm output power, which corresponds to the peak power of a 2-dBm average output power modulation, was 43 mA and no saturation was observed. The

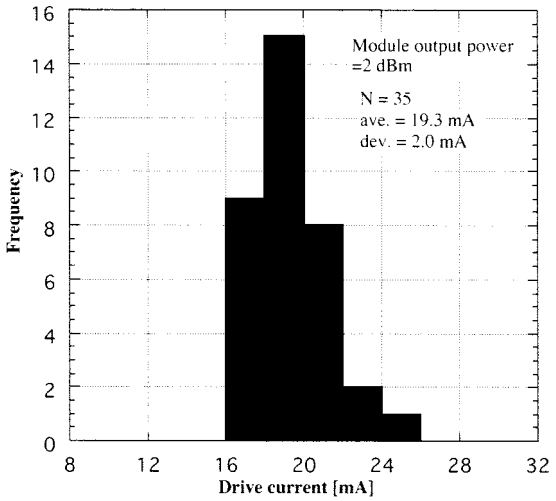

Fig. 10. Histogram of LD drive current.

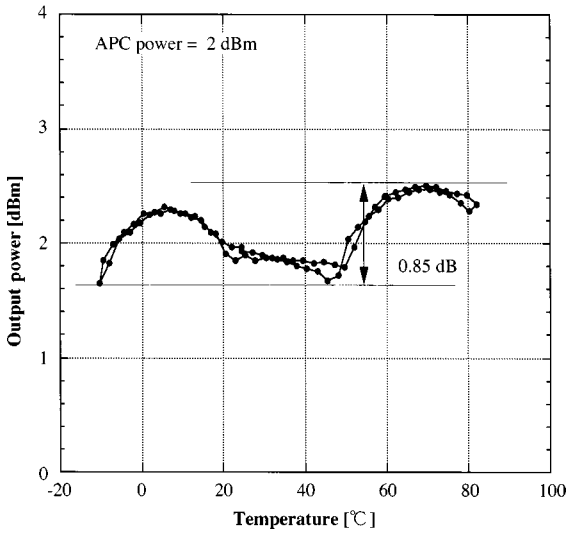

Fig. 11. Auto power control dependence on temperature.

fabrication yield for this module depends mainly on the accuracy of both the laser and the WDM filter assembly. In particular, there is a WDM filter loss for the reflection part, which is the LD side waveguide in this module (Fig. 2). We therefore confirmed the assembly yield by examining the LD drive current of 35 modules. Fig. 10 shows a histogram of the LD drive current during 2-dBm CW operation. The average current and the deviation were 19.3 and 1.99 mA, respectively. All optical modules needed a drive current of below 30 mA for 2 dBm CW operation. This indicates that the modules were modulated with a drive current of 40–60 mA for a 2-dBm average output power. We also measured the automatic power control characteristics of the module using an monitor M-PD. The monitoring current of the MPD was 0.8 mA when the module output power was 2 dBm. We set the monitoring current at 0.8 mA, and measured the output power deviation between -10 and 80°C. As shown in Fig. 11, the output power deviation was 0.85 dB throughout the temperature rang. We measured the responsivity and parasitic capacitance before bonding the module to the preamplifier. They were 0.65 A/W and 0.7 pF, respectively. The LD and PD

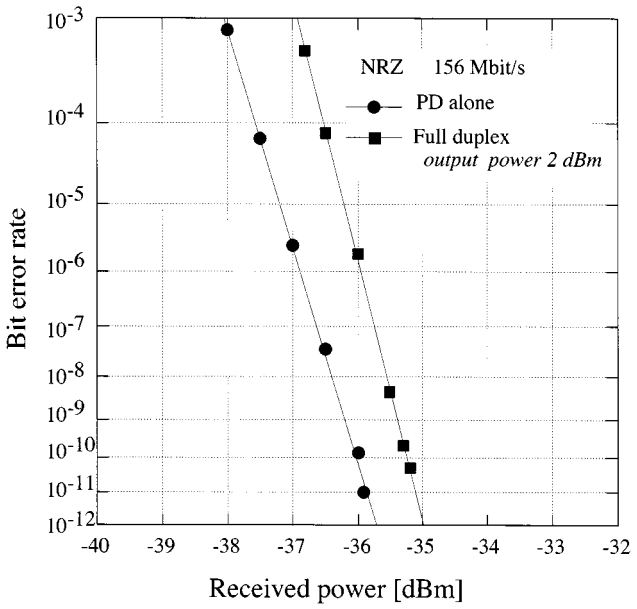

Fig. 12. Receiver performance.

coupling losses were estimated to be 3.9 and 0.9 dB, respectively, and this value means the estimated WDM filter insertion loss was less than 1 dB for the output light and almost negligible for the input light. The optical crosstalk was -44 dB.

We measured minimum sensitivity for 156 Mbit/s operation as shown in Fig. 12. Since our optical module configuration corresponds to that of the ONU for ATM-PON, we used a continuous 156 Mbit/s signal. The minimum sensitivity at a BER of 10^{-10} was -35.9 dBm without LD operation (circle). Even when the LD was operated at 156 Mbit/s with a 2 dBm average output power, we achieved a sensitivity of -35.2 dBm (square). The power penalty resulting from the simultaneous LD operation was only 0.7 dB. This value matches the power penalty estimated from Fig. 6 using the minimum sensitivity of -35.9 dBm without LD operation and the optical crosstalk noise power of -42 dBm (optical crosstalk of -44 dB and LD modulation power of 2 dBm). This indicates the crosstalk was well suppressed in this module.

VI. Conclusion

We developed a low crosstalk optical module. We achieved electrical and optical crosstalk values of -43 and -105 dB when the LD and PD were more than 9 mm apart. We evaluated the total crosstalk using the equivalent optical crosstalk of the electrical crosstalk and it was less than -43 dB with an LD-PD distance of 9 mm. We fabricated an optical module to examine the performance during full duplex operation with our module configuration. We measured the minimum sensitivity at a BER of 10^{-10} for 156 Mbit/s operation, and the module exhibited values of -35.9 and -35.2 dBm for receiver only and full duplex operation, respectively. This means that full duplex operation was successfully achieved with a compact optical module using a PLC platform.

These performance results confirm that hybrid integration technology can provide a compact, low crosstalk, and cost-effective optical module for optical subscriber systems.

APPENDIX I
CROSSTALK POWER AND MINIMUM SENSITIVITY

The BER β is described as

$$\beta = \frac{1}{2\sqrt{2\pi}} \int dX\, \rho(X) \left[\frac{1}{\sigma_1} \int_{-\infty}^{D} dS\, e^{-(S_1 - S + X)^2/(2\sigma_1^2)} + \frac{1}{\sigma_0} \int_{D}^{\infty} dS\, e^{-(S_0 - S + X)^2/(2\sigma_0^2)} \right] \quad (4)$$

where

S_j $(j = 0, 1)$ photo current level for a mark or space signal;
S and σ_j noise of the photo receiver system and its deviation;
X and $\rho(x)$ crosstalk current and its distribution;
D decision level [11]–[13].

When we assume that the crosstalk current distribution is a two-level Gaussian distribution as

$$\rho(X) = \frac{1}{2\sqrt{2\pi}\sigma_\chi} \left[\exp\left(-\frac{(X - \chi_1)^2}{2\sigma_\chi^2} \right) + \exp\left(-\frac{(X - \chi_0)^2}{2\sigma_\chi^2} \right) \right] \quad (5)$$

where χ_j is the crosstalk signal level and σ_χ is the deviation of the crosstalk signal, we obtain

$$\beta = \frac{1}{8} \left[\operatorname{erfc}\left(\frac{s + \chi - D}{\sqrt{2(\sigma^2 + \sigma_\chi^2)}} \right) + \operatorname{erfc}\left(\frac{D - \chi}{\sqrt{2(\sigma^2 + \sigma_\chi^2)}} \right) + \operatorname{erfc}\left(\frac{s - D}{\sqrt{2(\sigma^2 + \sigma_\chi^2)}} \right) + \operatorname{erfc}\left(\frac{D}{\sqrt{2(\sigma^2 + \sigma_\chi^2)}} \right) \right] \quad (6)$$

where we also assume that $\sigma_0 = \sigma_1 = \sigma$, $S_0 = \chi_0 = 0$, $S_1 = s$, $\chi_1 = \chi$. To simplify Eq. (6), we assume the additional conditions $\sigma_\chi \to 0$ and $D = (s + \chi)/2$. Then

$$\beta = \frac{1}{4} \left[\operatorname{erfc}\left(\frac{Q + q}{\sqrt{2}} \right) + \operatorname{erfc}\left(\frac{Q - q}{\sqrt{2}} \right) \right] \quad (7)$$

where $Q = s/(2\sigma)$ and $q = \chi/(2\sigma)$. Q and q corresponds to signal noise ratio and crosstalk noise ratio. Equation (7) indicates that Q for a fixed β is a function of q as $Q = Q(q; \beta)$. Therefore, the signal power penalty δP to satisfy β in a full duplex operation is determined as

$$\delta P = 10 \log_{10}\left(\frac{Q(q;\, \beta)}{Q(0;\, \beta)} \right) \quad \text{[dB]},$$

where we assume that the receiver PD is a pin-PD and the received current is proportional to the input power. The crosstalk noise ratio q is written as

$$q = \frac{Q_0 X}{P_{\min}}$$

where X is the crosstalk noise power, $Q_0 = Q(0;\, \beta)$, and $P_{\min}$ is the minimum sensitivity without LD operation. The unit of X and $P_{\min}$ is the watt. Using these relations, we estimate the minimum sensitivity for full duplex operation as

$$P_{\min}^{duplex} = P_{\min} + \delta P = P_{\min} + 10 \log_{10}\left(\frac{Q(Q_0 X/P_{\min};\, \beta)}{Q_0} \right). \quad (8)$$

Then the minimum sensitivity for full duplex operation $P_{\min}^{duplex}$ is expressed as a function of the minimum sensitivity without LD operation $P_{\min}$ and the crosstalk X. Fig. 6 shows this relation at a BER of 10^{-10}. When the crosstalk noise power is smaller than the minimum sensitivity without LD operation, where the ratio is about $1/Q(0;\, \beta) = 1/6.4 = -8$ dB, the power penalty is almost negligible. And when the crosstalk noise power is close to the minimum sensitivity without LD operation, the power penalty is close to 3 dB. This is because the system noise is negligible in this case and the optical crosstalk signal makes the signal level fluctuate and almost overlap the decision level.

ACKNOWLEDGMENT

The authors thank H. Kimura, M. Nakamura, and F. Hanawa for useful suggestions and technical support. They also thank A. Himeno, Y. Ohmori, and H. Toba for useful discussions and encouragement.

REFERENCES

[1] Y. Mochida, "Technologies for local-access fibering," *IEEE Commun. Mag.*, pp. 64–73, Feb. 1994.
[2] Y. Yamada, S. Suzuki, K. Moriwaki, Y. Hibino, Y. Tohmori, Y. Akatsu, Y. Nakazuga, T. Hashimoto, H. Terui, M. Yanagisawa, Y. Inoue, Y. Akahori, and R. Nagase, "Application of planar lightwave circuit platform to hybrid integrated optical WDM transmitter/receiver module," *Electron. Lett.*, vol. 31, no. 16, pp. 1366–1367, 1995.
[3] N. Uchida, Y. Yamada, Y. Hibino, Y. Suzuki, and N. Ishihara, "Low-cost hybrid WDM module consisting of a spot size converter integrated laser diode and a waveguide photodiode on a PLC platform for access network system," *IEICE Trans. Electron.*, vol. E80-C, no. 1, pp. 88–97, 1997.
[4] High speed optical access system based on passive optical network (PON) techniques, 1998.
[5] Y. Inoue, T. Oguchi, Y. Hibino, S. Suzuki, M. Yanagisawa, K. Moriwaki, and Y. Yamada, "Filter-embedded wavelength-division multiplexer for hybrid-integrated transceiver based on silica-based PLC," *Electron. Lett.*, vol. 32, no. 9, pp. 847–848, 1996.
[6] T. Hashimoto, Y. Nakasuga, Y. Yamada, H. Terui, M. Yanagisawa, Y. Akahori, Y. Tohmori, K. Kato, and Y. Suzuki, "Multichip optical hybrid integration technique with planar lightwave circuit platform," *J. Lightwave Technol.*, vol. 16, pp. 1249–1258, July 1998.
[7] H. Oohashi, M. Fukuda, Y. Kondo, M. Yamamoto, Y. Kadota, F. Ichikawa, Y. Kawaguchi, K. Kishi, Y. Sakai, M. Yanagisawa, S. Ishibashi, F. Hanawa, T. Hashimoto, Y. Tohmori, K. Yokoyama, Y. Itaya, and H. Toba, "Highly reliable and low-cost plastic modules of spot size converter integrated laser diode for access network," *ECOC'97*, pp. 351–354, 1997.
[8] K. Kato, M. Yuda, A. Kozen, Y. Muramoto, K. Noguchi, and O. Nakajima, "Selective-area impurity-doped planar edge-coupling waveguide photodiode (SIMPLE-WGPD) for low-cost, low-power-consumption optical hybrid modules," *Electron. Lett.*, vol. 7, no. 32, pp. 2078–2079, 1996.
[9] S. Mino, K. Yoshino, Y. Yamada, T. Terui, M. Yasu, and K. Moriwaki, "Planar lightwave circuit platform with coplanar waveguide for opto-electronic hybrid integration," *J. Lightwave Technol.*, vol. 13, pp. 2320–2326, Dec. 1995.
[10] M. Nakamura, N. Ishihara, H. Kimura, and H. Toba, "An 89 mW, 10 cc CMOS optical transceiver module for 50 Mb/x burst-mode communication," in *Proc. 8th Int. Workshop Opt./Hybrid Access Networks*, 1997, p. 12.

[11] R. G. Smith and S. D. Personick, "Receiver design for optical communication," in *Semiconductor Devices for Optical Communication*, H. Kressel, Ed. New York: Springer-Verlag, 1980, ch. 4.
[12] J. Conradi and R. Maciejko, "Digital optical receiver sensitivity degradation caused by crosstalk in bidirectional fiber optic systems," *IEEE Trans. Commun.*, vol. COM-29, p. 1012, 1981.
[13] T. Kanda, Y. Okano, K. Aoyama, and T. Kitami, "Design and performance of WDM transmission systems at 6.3 Mbits/s," *IEEE Trans. Commun.*, vol. COM-31, p. 1095, 1983.

Toshikazu Hashimoto, photograph and biography not available at the time of publication.

Takeshi Kurosaki, photograph and biography not available at the time of publication.

Masahiro Yanagisawa, photograph and biography not available at the time of publication.

Yasuhiro Suzuki (M'92), photograph and biography not available at the time of publication.

Yuji Akahori, photograph and biography not available at the time of publication.

Yasuyuki Inoue (M'94), photograph and biography not available at the time of publication.

Yuichi Tohmori (M'90), photograph and biography not available at the time of publication.

Kazutoshi Kato (M'93), photograph and biography not available at the time of publication.

Yasufumi Yamada, photograph and biography not available at the time of publication.

Noboru Ishihara, photograph and biography not available at the time of publication.

Kuniharu Kato (M'91), photograph and biography not available at the time of publication.